

REPORT

 OPEN ACCESS

Novel anti-Sialyl-Tn monoclonal antibodies and antibody-drug conjugates demonstrate tumor specificity and anti-tumor activity

Jillian M. Prendergast^a, Ana Paula Galvao da Silva^{a,*}, David A. Eavarone^{a,*}, Darius Ghaderi^{ib}^a, Mai Zhang^a, Dane Brady^b, Joan Wicks^b, Julie DeSander^a, Jeff Behrens^a, and Bo R. Rueda^{c,d}

^aSiamab Therapeutics, Inc., Newton, MA, USA; ^bAlizée Pathology, LLC, Thurmont, MD, USA; ^cVincent Center for Reproductive Biology, Department of Obstetrics and Gynecology, Massachusetts General Hospital, Boston, MA, USA; ^dHarvard Medical School, Boston, MA, USA

ABSTRACT

Targeted therapeutics that can differentiate between normal and malignant tumor cells represent the ideal standard for the development of a successful anti-cancer strategy. The Sialyl-Thomsen-nouveau antigen (STn or Sialyl-Tn, also known as CD175s) is rarely seen in normal adult tissues, but it is abundantly expressed in many types of human epithelial cancers. We have identified novel antibodies that specifically target with high affinity the STn glycan independent of its carrier protein, affording the potential to recognize a wider array of cancer-specific sialylated proteins. A panel of murine monoclonal anti-STn therapeutic antibodies were generated and their binding specificity and efficacy were characterized *in vitro* and in *in vivo* murine cancer models. A subset of these antibodies were conjugated to monomethyl auristatin E (MMAE) to generate antibody-drug conjugates (ADCs). These ADCs demonstrated *in vitro* efficacy in STn-expressing cell lines and significant tumor growth inhibition in STn-expressing tumor xenograft cancer models with no evidence of overt toxicity.

ARTICLE HISTORY

Received 16 December 2016
Revised 25 January 2017
Accepted 30 January 2017

KEYWORDS

Antibody Drug Conjugate (ADC); breast cancer; CD175s; colon cancer; ovarian cancer; sialyl-Tn; STn; Tumor-Associated Carbohydrate Antigen (TACA)

Introduction

Cancer is the second leading cause of death in the US, with 595,690 deaths and 1.69 million new cases expected in 2016.¹ A targeted therapy that reliably differentiates between normal and malignant tumor cells represents the gold standard for cancer treatment. Glycosylation of proteins is one of the most abundant and diverse post-translational modifications, with more than half of all human proteins estimated to be glycosylated.² Aberrant glycosylation has been implicated in an array of human diseases and is a common feature of cancer cells.^{3,4} One altered glycosylation pathway associated with malignancy is O-glycan biosynthesis. Incomplete O-glycosylation results in truncated glycans, such as Thomsen-nouveau (Tn; GalNAc- α 1-O-Ser/Thr) antigen and its sialylated version sialyl-Tn (STn; Sia α 2-6GalNAc- α 1-O-Ser/Thr, also known as CD175s). Aberrant STn expression is associated with dysregulation of the O-glycosylation machinery, including imbalanced expression of molecular chaperone Cosmc/T-synthase and STn synthase (ST6GalNAc-I). Cosmc is a chaperone of T-synthase and both are necessary for the addition of glycan structures to Tn in mucin-type core-1 O-glycans.⁵ STn synthase is an α 2,6-sialyltransferase that catalyzes the transfer of a terminal sialic acid to Tn, effectively capping O-glycans and preventing any further glycan additions. *De novo* STn expression via STn synthase transfection can change a tumor's malignant phenotype,


leading to more aggressive cancer cell behaviors.⁶⁻⁹ Truncated O-glycans are one class of tumor-associated carbohydrate antigens (TACAs)¹⁰⁻¹² that can be targeted by cancer therapy, particularly when presented on cell surface glycoproteins.

STn is expressed in numerous human adenocarcinomas, including breast, ovarian, bladder, cervical, colon, pancreatic and lung cancers.^{3,5,13-15} The presence of cell surface/membrane STn in tumors is associated with tumorigenesis, metastatic potential, immune suppression, chemoresistance and poor prognosis;^{3,14,16} therefore, STn is an attractive therapeutic target. Therapeutic approaches targeting STn have consisted primarily of STn vaccines. The most advanced clinical candidate was Theratope, a therapeutic vaccine consisting of STn coupled to keyhole limpet hemocyanin (KLH). In murine mammary carcinoma models, Theratope immunization induced a potent antibody response that delayed tumor growth.¹⁷ However, Theratope failed to achieve its primary end point in a Phase 3 clinical trial not due to toxicity but to lack of efficacy in part possibly due to the broad variability of STn expression in breast cancer tissues.^{3,18}

TACAs are poorly immunogenic, and thus making effective vaccines or antibodies against these targets has proven difficult.¹⁴ Previous antibody development efforts used purified glycoproteins from cancer samples and Freund's adjuvant, or mucin-coated heat-inactivated bacteria, for mouse immunization. These approaches have resulted in the development of

CONTACT Jillian M. Prendergast  jill@siamab.com  90 Bridge St. Suite 100, Newton, MA 02458, USA.

*These authors contributed equally to this work.

 Supplemental data for this article can be accessed on the publisher's website.

Published with license by Taylor & Francis Group, LLC. © Siamab Therapeutics, Inc.

This is an Open Access article distributed under the terms of the Creative Commons Attribution-NonCommercial-NoDerivatives License (<http://creativecommons.org/licenses/by-nc-nd/4.0/>), which permits non-commercial re-use, distribution, and reproduction in any medium, provided the original work is properly cited, and is not altered, transformed, or built upon in any way.

several murine anti-STn monoclonal antibodies (mAbs), including B72.3¹⁹ (and its successor antibody CC49²⁰), TKH2,²¹ and HB-STn1(clone 3F1^{21,22}), and others.¹⁴ The target specificity of these mAbs have come into question as these mAbs bind additional glycan targets and may have glycoprotein preferences for antigen recognition.²³ Advances in adjuvant technology and immunization strategies have enabled high titer and desirable antibody maturation responses to historically difficult immunization targets.²⁴ We used immune modulatory and enhanced delivery of a TLR9 agonist (CpG oligodeoxynucleotides) and AbISCO, an adjuvant composed of saponin, phospholipid and cholesterol that acts both as an immunostimulant and delivery agent. These immunization optimization strategies and synergistic adjuvants (AbISCO-100 and ODN 2395) enabled the generation of high affinity, STn-specific mAbs.

Antibody-drug conjugates (ADCs) utilize a mAb as a targeting tool for delivering a potent cytotoxic payload specifically to cancer cells. An STn-specific ADC may overcome shortcomings of previous attempts to target STn with therapeutic vaccines. ADCs enable dosing at therapeutic concentrations, do not rely on variable immune system responses, and additionally offer the promise of companion diagnostic development to identify patients most likely to benefit from therapy. The specificity and targeting capabilities of ADCs have resulted in numerous drugs with clinical efficacy and favorable safety profiles.²⁵⁻²⁷ We used the microtubule disrupting agent monomethyl auristatin E (MMAE) with a MC-vc-PAB linker system, which has been demonstrated effective in killing tumor antigen expressing cells *in vitro* along with neighboring negative tumor cells through bystander killing,²⁸ and successful *in vivo* and human clinical studies, leading to the Food and Drug Administration (FDA)'s approval of the product brentuximab vedotin (Adcetris®).^{29,30} Here, we report the development of novel

ADCs consisting of anti-STn mAbs, conjugated to MMAE, which demonstrate high affinity, specificity and anti-tumor activity *in vitro* and *in vivo*.

Results

Antibody specificity and epitope mapping

Generating high specificity and affinity anti-STn mAbs depends on the ability to precisely profile the glycan binding specificities of candidate antibodies, independent of the protein carrier. We developed a glycan array in collaboration with Dr. Ajit Varki³¹ that contains 71 chemically synthesized and well-characterized glycans (Table S1). The glycan array includes several STn-related structures, allowing determination of the exact binding epitope of each antibody (Fig. 1). The information generated from the glycan array, and other binding assays, enables us to determine the precise specificity of the anti-STn antibodies generated and identify antibodies that do not cross-react with related glycans present in the glycan array.

The glycan array technology utility was demonstrated by characterization of commercially available anti-STn mAbs. The binding epitope for these mAbs is purported to be 'Neu5Ac- α -2,6-galNAc' (as per manufacturer's description). However, commercial mAbs recognize multiple STn-related oligosaccharides including the Tn antigen (GalNAc) (Fig. 2). Anti-STn antibody 3H1951 did not recognize STn or Tn structures, but instead bound Neu5,9Ac2-ST/Neu5Gc-ST (Neu5Gc α 3Gal β 3GalNAc/Neu5,9Ac2 α 3Gal β 3GalNAc). In contrast, our internally generated anti-STn mAb 8C2-2D6 selectively binds to STn, but no related structures (Fig. 2). Additionally, we used flow cytometry and enzyme-linked immunosorbent assays (ELISA) to map the antibodies' binding epitope and determine relative affinities. We tested for sensitivity to mild periodate

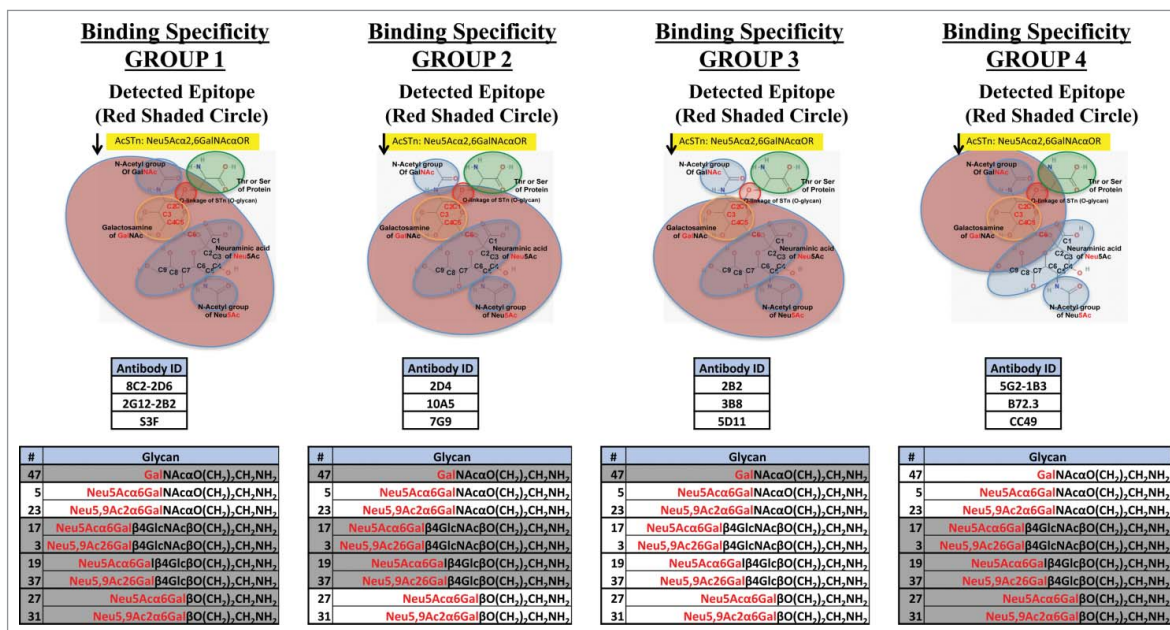


Figure 1. Binding groups determined for anti-STn antibodies. mAbs were grouped based on their binding specificities toward O-glycans. Group 1: mAbs bind STn only (Neu5Ac α 2,6GalNAc α O). Group 2: mAbs bind to Neu5Ac α 2,6Gal(NAc) α O. Group 3: mAbs bind to Neu5Ac α 2,6Gal(NAc) α O and Neu5Ac α 2,6Gal(NAc) β 1,4Glc(NAc) β O. Group 4: mAbs bind to STn and Tn (GalNAc α O). All mAbs also bind the corresponding 9-O-acetylated and Neu5Gc O-glycans. The red shaded circles in the figure and non-greyed out glycans in the table represent the detected epitope for each group.

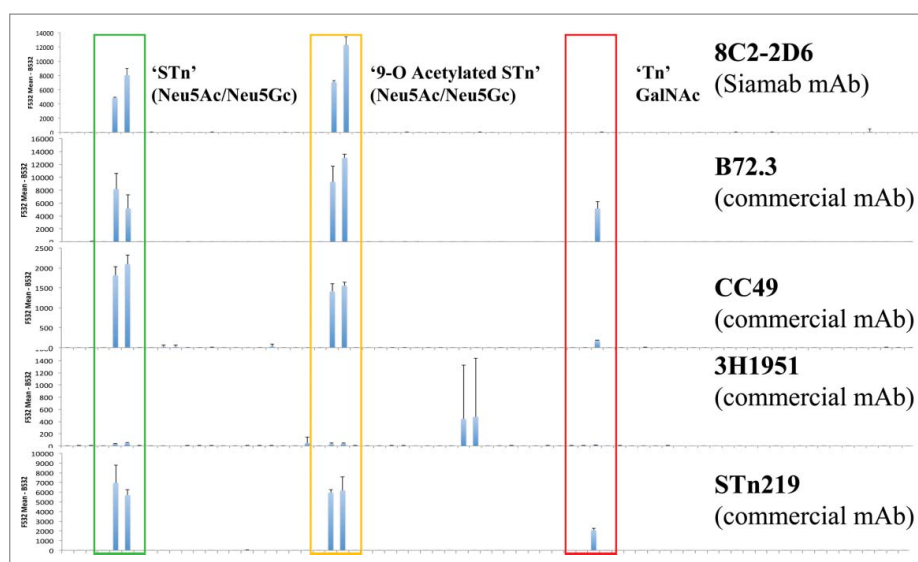


Figure 2. Representative binding profiles of anti-STn antibodies on the glycan array. Anti-STn commercial antibodies were purchased from vendors (B72.3 Thermo Scientific; CC49 and 3H1951, Santa Cruz Biotechnology; STn219 Abcam). All antibodies were tested using 1 μ g/mL concentration. Commercial antibodies recognize multiple STn-related oligosaccharides including the Tn antigen (GalNAc).

treatment to determine whether the antibodies bound to the side chain of terminal sialic acids. This periodate oxidation of terminal sialic acids removes the side chain, giving rise to the C-7 analogs of these sialic acids.³² The commercially available mAbs B72.3 and CC49 bound equally well to mucins after periodate treatment, suggesting that the binding of these mAbs does not rely on the side chain nor acetylation of sialic acid.

Together, ELISA, flow cytometry and glycan arrays were used to characterize the binding of the panel of 8 anti-STn mAbs. The results from ELISA and flow cytometry demonstrated nanomolar EC50s, suggesting robust binding affinity (Table 1). The glycan binding profile determined from the glycan array further demonstrated STn specific binding for most mAbs tested.

Generation and characterization of anti-STn candidate mAbs

Six to eight-week-old female mice (BALB/c) were immunized subcutaneously (50 μ L per site, 4 sites, 200 μ L/mouse) on days 0, 14, 28 and 42 with immunogen and an adjuvant cocktail (AbISCO-100 and ODN 2395). Blood was collected before each

immunization, including the final boost. Sera was screened with ELISAs and glycan arrays to identify mice with desirable anti-STn binding profiles, and to identify optimal timing for splenic collection. Splenocytes were harvested and fused to establish hybridomas and an anti-STn mouse antibody panel. Hybridomas were generated and screened for specificity and affinity to STn antigen by FACS, ELISA and glycan array. Selected hybridomas were expanded for antibody production and cell pelleted for protein sequencing. Antibodies were purified and in some cases made recombinantly to enhance production, purification and analysis. An example of the evolution of the anti-STn antibody response leading to candidate 2G12-2B2 is represented in Fig. 3. Additionally, serum ELISA immune responses are detailed in Table S2. A robust panel of mAbs was narrowed to 8 for full binding characterization (Table 1).

Immunohistochemistry to confirm cancer specificity

Tissue microarrays (TMAs) consisting of a panel of formalin-fixed neoplastic and normal tissues were stained with anti-STn mAbs to determine reactivity with neoplastic and normal cells.

Table 1. Anti-STn mAb binding results summary.

| mAb | Isotype | ELISA EC50 (nM) | | | Glycan Array | | FACS EC50 (nM) MDA-MB-231 STn+ | Internalization | |
|------------------|---------|------------------|------------------|------------------|------------------|----------------------------|-----------------------------------|-----------------|---------|
| | | BSM ¹ | OSM ² | PSM ³ | (%) ⁴ | Binding Group ⁵ | | Mean FI | p-value |
| 8C2-2D6 | IgG2a,k | 0.4 | 0.5 | 0.3 | 99 | 1 | 2.8 | 7.6 | 0.03 |
| 2G12-2B2 | IgG2a,k | 0.1 | 0.1 | 0.1 | 99 | 1 | 0.3 | 6.7 | 0.01 |
| 4G8-1E3 | IgG2a,k | 1.2 | 0.6 | 0.1 | 99 | 1 | 0.7 | 7.4 | 0.01 |
| S3F [*] | IgG2a,k | 0.3 | 0.1 | 0.2 | 98 | 1 | 3.1 | 8.1 | 0.001 |
| 5G2-1B3 | IgG1,k | 0.4 | 0.2 | 10.2 | 92 | 4 | 0.2 | ND | ND |
| 2C2-2C5 | IgG3,k | 1 | 0.2 | 0.2 | 100 | 1 | 0.8 | 6.2 | 0.03 |
| 5E6-2E7 | IgG3,k | 5.8 | 0.8 | 0.4 | 100 | 1 | 1.8 | 7.5 | 0.04 |
| 9F11-1F7 | IgG3,k | 4.6 | 0.9 | 0.9 | 99 | 1 | 0.8 | 5.5 | 0.05 |

Summary Table of binding results.

¹BSM is bovine submaxillary mucin. ²PSM is Porcine Submaxillary Mucin. ³OSM is ovine submaxillary mucin. ⁴% signal on the glycan array; the higher the percentage the more STn specific the antibody. ⁵The binding group see Fig. 1. ND is not determined. ELISA EC50s were determined after subtracting signal from periodate treated wells from non-treated wells. *S3F was not generated during our immunizations – this is derived from HB-STn clone 3F1. We class switched from mouse IgG1 and recombinantly expressed as a mouse IgG2a, we refer to this engineered antibody as “S3F” in the text.

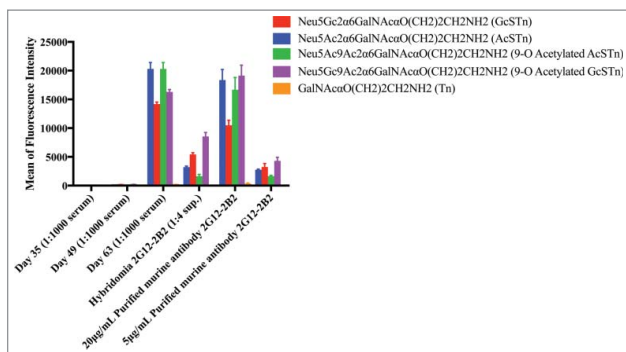


Figure 3. Immunization resulted in STn specific antibodies as seen in sera and purified hybridoma supernatants. Immune response and antibody evolution from a single animal demonstrated significant and specific STn binding. The antibody binds to all 4 variants of STn included on the array (Neu5Ac/Gc and 9-O acetylated forms). Antibody generation was monitored in serum after immunization (Day 35, 49 and 63) using the glycan array. STn-specific antibodies were observed starting on Day 63, no significant binding was observed to non-STn glycans. This mouse was used to generate hybridomas and clone 2G12–2B2 was selected for STn specificity. Purified antibodies from this hybridoma supernatant demonstrated significant and specific STn binding on the glycan array.

Optimal immunohistochemistry (IHC) staining conditions were determined and validated on appropriate STn-positive and STn-negative control cells and tissues before testing on TMAs (data not shown). The IHC-stained TMAs were evaluated and scored for cell type, subcellular localization, and staining intensity and frequency by a board-certified pathologist (JW) with extensive experience in immunohistochemical analysis. The specific reactivity of candidate anti-STn mAbs was evaluated across 13 different tumor types and 30 normal tissues (Table 2). For a given tissue, the staining patterns for all anti-STn mAbs tested were similar in terms of cell type and subcellular location (e.g., cytoplasm versus membrane), and differed by intensity and frequency of staining. There was infrequent membrane staining of the normal, non-neoplastic tissue. Any staining observed in normal tissues was generally cytoplasmic, or involved staining of apical membranes. Neither of these locations are expected to be readily accessible to anti-STn ADCs in the circulation. In comparison, there was positive membrane reactivity (not limited to apical membranes) across

a broad range of human epithelial cancers. Examples of 2G12–2B2 staining of normal tissue and neoplastic lung, pancreas and colon tissue are detailed in Fig. 4. Urinary bladder and ovarian cancer also yielded a strong membrane staining pattern with high frequency. A summary of positive IHC-scored neoplastic TMA cores with the other 7 mAbs tested is shown in Table 2.

In vitro internalization assays

To determine whether anti-STn mAbs were internalized upon binding to the cell surface, and therefore candidates for cytotoxic payload conjugation, all mAbs were tested for internalization in STn-expressing human breast cancer cells. Eight anti-STn mAbs and an isotype control were conjugated to a pH reactive dye per manufacturer's recommendations (pHAb Reactive Dye, Promega catalog number G9845). This dye becomes fluorescent only upon internalization into lower pH organelles such as lysosomes. Six of eight mAbs (S3F, 4G8–1E3, 2G12–2B2 $P < 0.01$; 8C2–2D6, 2C2–2C5, and 5E6–2E7 $P < 0.05$) showed significant internalization into STn-expressing MDA-MB-231 cells as compared with non-expressing cells (Fig. 5A, Table 1). Poor 5G2–1B3 recovery after conjugation did not allow for comparison to other tested mAbs. The isotype control MOPC173 mAb did not internalize ($p > 0.05$) into either STn+ or STn- cells.

Internalization also was examined using an Alexa 488-labeled S3F antibody in STn-expressing and non-expressing MDA-MB-231 cells. The Alexa 488-labeled S3F antibody only stained STn+ cells and optimal staining was achieved with 5 $\mu\text{g}/\text{mL}$ (Fig. 5B). Internalization appeared as early as 15 minutes and was strongly evident at 60 minutes.

ADC conjugation and in vitro viability assays

Effects of unconjugated and MMAE-conjugated mAbs on cell viability were compared in both transfected STn-expressing (STn+) and parental (STn-) MDA-MB-231 human breast cancer cell lines. While the MMAE-conjugated isotype control mAb had no effect on cell viability, MMAE-conjugated

Table 2. Binding specificity of antibody panel on human TMA.

| | | | | | | | |
|------------------|------|------------------|------|------------------|------|------------------|------|
| <u>S3F</u> | | <u>4G8–1E3</u> | | <u>8C2–2D6</u> | | <u>5G2–1E3</u> | |
| Ovarian: | 3/9 | Ovarian: | 5/9 | Ovarian: | 4/9 | Ovarian: | 2/9 |
| Urinary bladder: | 5/9 | Urinary bladder: | 3/9 | Urinary bladder: | 3/9 | Urinary bladder: | 2/9 |
| Colorectal: | 7/9 | Colorectal: | 7/9 | Colorectal: | 6/9 | Colorectal: | 7/9 |
| Pancreatic: | 9/10 | Pancreatic: | 8/10 | Pancreatic: | 8/10 | Pancreatic: | 7/10 |
| Lung: | 2/2 | Lung: | 2/2 | Lung: | 2/2 | Lung: | 1/2 |
| Stomach: | 9/10 | Stomach: | 9/10 | Stomach: | 9/10 | Stomach: | 2/10 |
| <u>5E6–2E7</u> | | <u>2G12–2B2</u> | | <u>9F11–1F7</u> | | <u>2C2–2C5</u> | |
| Ovarian: | 1/9 | Ovarian: | 5/9 | Ovarian: | 1/9 | Ovarian: | 2/9 |
| Urinary bladder: | 2/9 | Urinary bladder: | 3/9 | Urinary bladder: | 1/9 | Urinary bladder: | 1/9 |
| Colorectal: | 5/9 | Colorectal: | 7/9 | Colorectal: | 4/9 | Colorectal: | 5/9 |
| Pancreatic: | 6/10 | Pancreatic: | 6/10 | Pancreatic: | 3/10 | Pancreatic: | 7/10 |
| Lung: | 1/2 | Lung: | 2/2 | Lung: | 0/2 | Lung: | 0/2 |
| Stomach: | 6/10 | Stomach: | 8/10 | Stomach: | 2/10 | Stomach: | 5/10 |

Antibody candidates' staining of tumor cells is presented as a fraction of stained TMA from total TMAs tested. Thirteen common tumor types were tested, of these ovarian, urinary bladder, colorectal, pancreatic, lung and stomach are described in Table 2. Neoplastic subtypes as follows: ovarian was a combination of serous (8) and mucinous (1) adenocarcinoma; urinary bladder transitional cell carcinoma; colorectal adenocarcinoma well (2) and moderately (7) differentiated; pancreas ductal adenocarcinoma moderately differentiated; lung adenocarcinoma well differentiated; stomach was a combination of adenocarcinoma poorly (5), moderately differentiated (2), signet ring cell carcinoma (1), and mucinous adenocarcinoma (1).

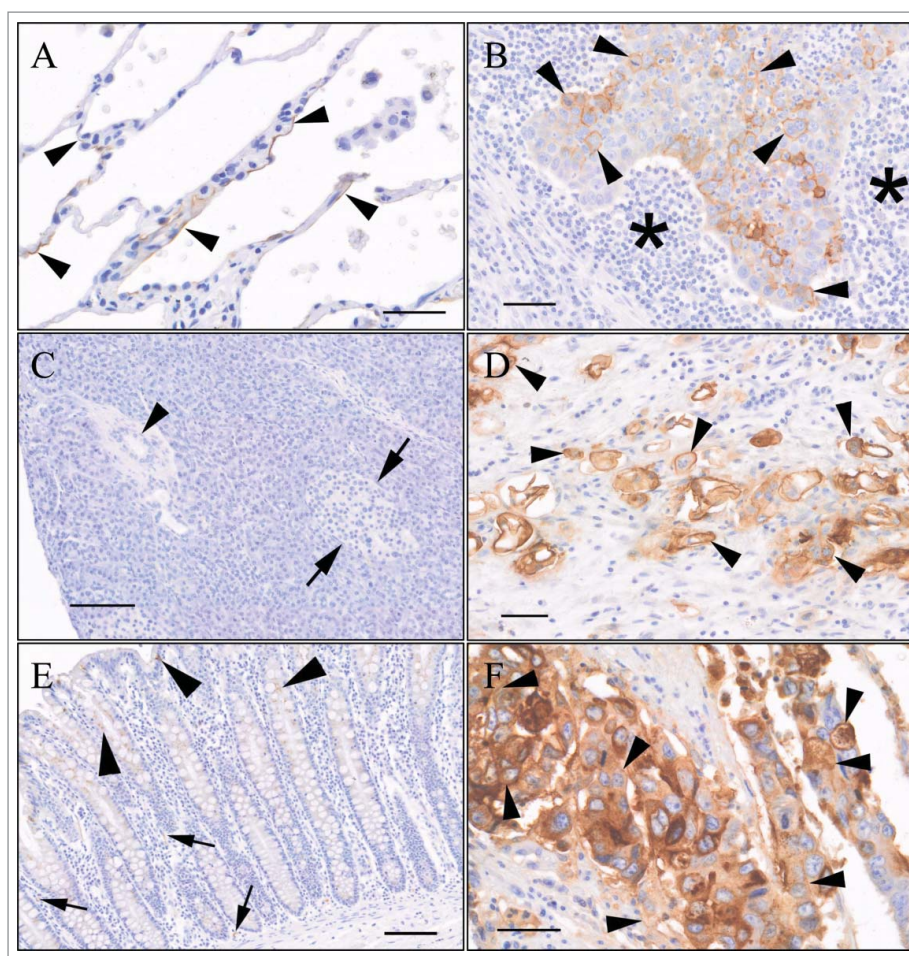


Figure 4. Binding specificity of 2G12-2B2 on human TMAs. (A) Normal (non-neoplastic) lung: There was lumen membrane staining of rare alveolar lining cells (arrowheads). Image is from a region with more frequent staining. Bar = 40 μm . (B) Lung squamous cell carcinoma: Membrane staining of neoplastic epithelial cells (arrowheads). Asterisks indicates mononuclear inflammatory cell infiltrate around neoplastic cell infiltrate. Bar = 100 μm . (C) Normal (non-neoplastic) pancreas: There was no staining of any tissue elements. Arrows = islet of Langerhans. Arrowhead = Pancreatic ductule. Bar = 100 μm . (D) Pancreatic ductal adenocarcinoma: Moderate to intense staining of neoplastic cells infiltrating into adjacent stroma. Bar = 50 μm . (E) Normal (non-neoplastic) colon: Cytoplasmic staining of goblet cells (arrowheads). Cytoplasmic +/- membrane staining of scattered endothelial cells. Bar = 100 μm . (F) Ascending colon adenocarcinoma, moderately differentiated: Frequent membrane and staining of neoplastic epithelial cells (arrowheads). Cytoplasmic staining also present. Bar = 40 μm .

anti-STn mAbs induced cell death of STn+ MDA-MB-231 cells (Fig. 6). Four of 5 MMAE-conjugated anti-STn mAbs had single digit nanomolar IC₅₀ values. No cell death was observed when parental STn- MDA-MB-231 cells were treated with MMAE-conjugated, nor when STn+ MDA-MB-231 cells were treated with unconjugated anti-STn mAbs (Fig. S1).

ADC efficacy and safety in an *in vivo* human breast cancer model

Three anti-STn ADCs (S3F-, 2G12-2B2- and 4G8-1E3-CL-MMAE) were evaluated as single agents in ICR SCID mice implanted subcutaneously with STn+ MDA-MB-231. MOPC173-CL-MMAE was used as an ADC isotype control. Unconjugated antibody was an equal mixture of 2G12-2B2 and 4G8-1B3. All antibodies were tested at 2.5 mg/kg final concentration. In addition to evaluating the efficacy of these ADCs, body weight was monitored as an indicator of toxicity, with a decrease of > 5% considered significant. Tumor volumes were plotted in Fig. 7, and inhibition of tumor growth was expressed

as percent mean treated tumor volume/mean vehicle control tumor volume (%T/C) (error bars = SEM).

On Day 22, the vehicle control group was killed after it met the group mean tumor volume end point of 1000 mm³, at which time the unconjugated mAb treatment produced a 60.0% T/C ($p = 0.1$). At the same time point, isotype control ADC MOPC173-CL-MMAE showed 16.0% T/C ($p = 0.001$), indicating that the payload itself had some anti-tumor activity. This may be due to binding of the isotype control to unknown target(s) *in vivo*, or could indicate an effect of some toxin is being shed in the system. The anti-STn ADCs 4G8-1E3- and 2G12-2B2-CL-MMAE were the most robust treatments, with 3.6% and 3.0% T/C, respectively (both $p < 0.001$). Significant differences between isotype control MOPC173-CL-MMAE and 2G12-2B2- ($p = 0.003$) and 4G8-1E3-CL-MMAE ($p = 0.004$) were also observed on Day 22. No significant difference was observed between S3F-CL-MMAE and MOPC173-CL-MMAE isotype control on Day 22. S3F-CL-MMAE anti-STn ADC demonstrated modest inhibition (11.0% T/C ($p < 0.001$)). On day 43, 4 weeks after the last ADC dose was administered, mean tumor volumes in the MOPC173- and S3F-CL-

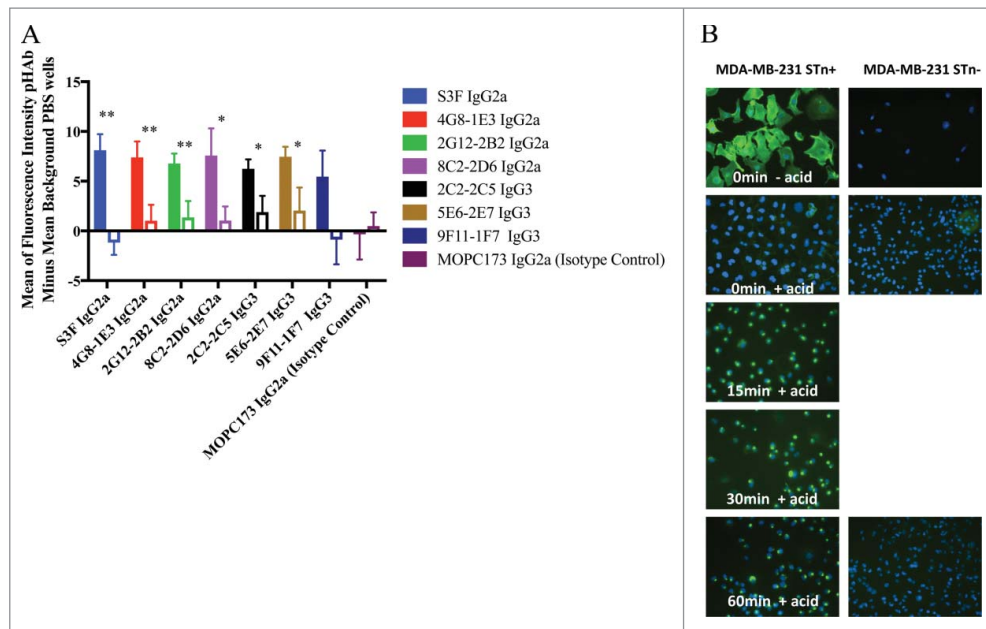


Figure 5. Internalization of STn antibodies in STn± MDA-MB-231 cells. (A) Internalization of labeled anti-STn mAbs were tested using STn-expressing (filled bars) and non-expressing (empty bars) human breast cancer cells. Eight anti-STn mAbs and an isotype control were conjugated to a pH reactive dye that becomes fluorescent upon internalization into lower pH organelles like lysosomes. Six of eight mAbs showed significant internalization into STn-expressing cells as compared with non-expressing cells ($^*P < 0.05$, $^{**}P < 0.01$, $N = 6$). 5G2-1B3 was also conjugated, but poor recovery after conjugation did not allow for comparison to other tested antibodies. The isotype control MOPC173 antibody did not significantly internalize into either expressing or non-expressing cells. Error bars denote standard error. P-values were determined by one-sided student-t test with unequal variance. (B) Representative images for antibody Alexa 488-labeled S3F internalization. Cells were incubated with 5 μ g/mL S3F-Alexa 488 for 1 hour at 4°C, then incubated at various times at 37°C (0, 15, 30, 60 minutes). Cells were treated with 5-minute acid wash (150 mM NaCl/HCl pH 2.5) to remove surface bound antibodies. No surface staining nor internalization were seen in MDA-MB-231 STn- cells. Internalization of S3F was seen in STn+ cells as early as 15 minutes and was strongly evident at 60 minutes.

MMAE-treated groups increased to ~ 850 mm³, while the groups treated with the 4G8-1E3- and 2G12-2B2-CL-MMAE exhibited suppressed mean tumor volumes of 97 and 146 mm³, respectively. Effect of treatment on average body weight for each of the treatment groups (Fig. S2) showed no overt signs of toxicity in any of the control or treated groups. While the mean body weight loss observed temporarily spiked to a maximum of -1.8 to -2.5% for the ADC and unconjugated mAbs after the first dose, these mice recovered by the second dose.

Anti-STn ADC efficacy in a non-transfected human colorectal cancer model

We have identified several cell lines by flow cytometry that naturally express STn without requiring transfection. STn

expression levels of these cell lines compared with transfected lines is detailed in Table 3. Approximately 60% of cultured COLO205 cells express STn on the cell surface in *in vitro* monolayer culture ($EC_{50} = 10$ nM). A preliminary xenograft study using the COLO205 cell line and the anti-STn ADC is shown in Fig. 8. The anti-STn ADC S3F-CL-MMAE demonstrated significant tumor growth inhibition (%T/C 44.5%, $p = 0.008$) *in vivo* compared with the other 3 treatment groups.

Discussion

STn is known to be expressed by more than 80% of human carcinomas, including pancreatic, ovarian, and colorectal cancers.³

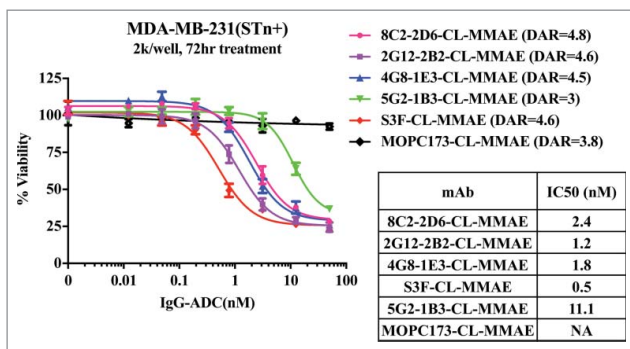


Figure 6. Cell viability assay with mouse anti-STn ADCs. Anti-STn ADC antibodies kill STn+ MDA-MB-231 cells (single digit nanomolar IC50s), while naked anti-STn antibodies do not (Fig. S1).

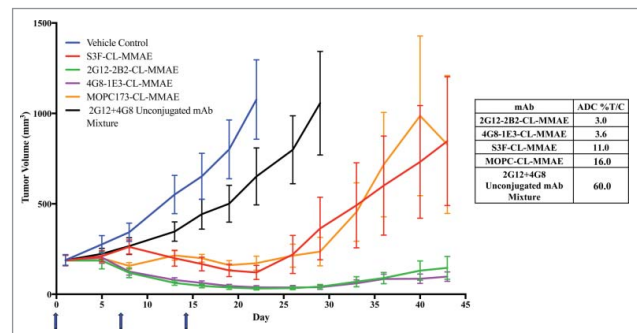


Figure 7. Effect of anti-STn ADCs on tumor growth in subcutaneous human breast cancer xenograft model. An ICR SCID subcutaneous xenograft mouse model was used with MDA-MB-231 STn+ transfected human breast cancer cells. The dosing schedule was Q7Dx3 (one 2.5 mg/kg dose a week for 3 weeks, blue arrows). When tumors reached end point volume (≥ 1000 mm³) the group was terminated. $N = 10$ mice for all groups. Unconjugated antibody control was an equal mixture of 2.5 mg/kg unconjugated 2G12-2B2 and 4G8-1E3.

Table 3. STn expression in various cancer cell lines.

| Naturally STn- lines stably transfected with ST6GalNAc-I cDNA to express STn | | |
|--|------------|-------------------------|
| % STn Expression | Cell Line | Tumor Type |
| 98.7 | MDA-MB-231 | Human Breast |
| | STn+ | Adenocarcinoma |
| 90.0 | SKOV3-H | Human Ovarian Carcinoma |
| | | High Expressing Line |
| 50.0 | SKOV3-M | Human Ovarian Carcinoma |
| | | Medium Expressing Line |
| 20.0 | SKOV3-L | Human Ovarian Carcinoma |
| | | Low Expressing Line |
| Naturally STn + lines: Expression Naturally Varies from High to Low | | |
| % STn Expression | Cell Line | Tumor Type |
| 99.5 | OV-90 | Human Ovarian Carcinoma |
| 79.4 | SNU-16 | Human Gastric Carcinoma |
| 75.0 | OVCAR8 | Human Ovarian Carcinoma |
| 69.9 | LS174T | Human Colon Carcinoma |
| 67.7 | COLO-205 | Human Colon Carcinoma |
| 35.0 | OVCAR3 | Human Ovarian Carcinoma |
| 28.9 | Jurkat | Human T Cell Leukemia |
| 26.4 | OVCAR4 | Human Ovarian Carcinoma |
| 20.0 | OVCAR5 | Human Ovarian Carcinoma |

%STn expression was determined using S3F antibody and flow cytometry of cultured cells, STn+ cells were indicated as a % of total cells in the table above.

De novo expression of STn via STn synthase (α 2,6-sialyl-transferase) transfection has been reported to lead to more malignant phenotypes.⁶⁻⁹ Normal adult tissue expression of STn is rare and largely restricted to cell types specialized in secretion, generally on the apical surface, which would likely restrict its accessibility to anti-STn ADCs administered in the blood.³

Historically, glycans have been difficult targets to raise a robust immune response against.^{14,33} We have completed multiple rounds of mouse STn immunization to optimize the immunogen and adjuvant selected. In previous immunization attempts, we used various mouse strains, synthetic glycan and mucin-based immunogens, and traditional adjuvants (CFA/IFA), which resulted in few glycan-specific antibody candidates. In our most successful immunizations, we immunized using various intact and digested mucins with newer adjuvants (ODN and AbISCO). Intact mucins produced a more robust

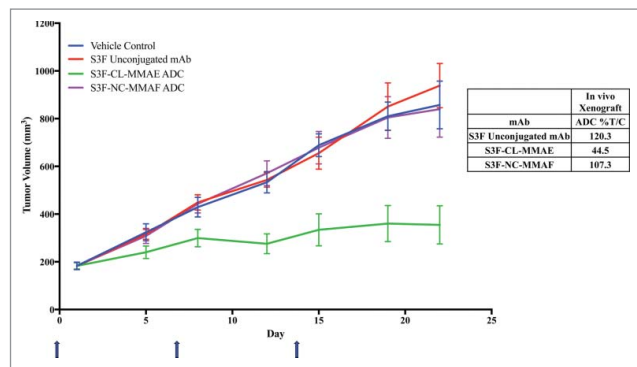


Figure 8. Proof-of-concept human colorectal cancer naturally expressing STn model using anti-STn S3F and 2 different ADC formats. An athymic nude mouse subcutaneous xenograft mouse model was used with COLO205 human colorectal cancer cells. Animals were dosed Q7Dx3 at 5 mg/kg (one 5 mg/kg dose a week for 3 weeks, blue arrows). Antibody alone with no toxin (red), S3F-CL-MMAE (MC-vc-PAB-MMAE, green) and S3F-NC-MMAF (NC-MMAF, purple), all were compared with vehicle alone (blue).

immune response and generated glycan target-specific antibodies. The combination of these immunogens and adjuvants resulted in a more robust immune response and the discovery of glycan target-specific antibodies.

Attempts to target the STn antigen have included both vaccine- and antibody-based approaches. The most advanced agent targeting STn was a vaccine (Theratope), which was evaluated in breast cancer patients in a Phase 3 clinical trial that concluded in 2003.³⁴ The anti-STn mAbs B72.3 and CC49 also were tested in the clinic; while these mAbs are described as specific to the STn-glycoprotein TAG-72, they also cross react with the non-sialylated glycan, Tn.^{3,35} Oncoscint[®] (B72.3 antibody conjugated to indium-111) was approved by FDA as a diagnostic in 1992³⁶ for whole body imaging for recurrences of ovarian and colorectal cancers. While Oncoscint[®] was found to be safe and effective in detecting tumors, this product was eventually discontinued due to PET (positron emission tomography) technology advancements in detecting metastatic lesions.³⁷ The regulatory approval and strong safety profile of Oncoscint[®]³⁸ led to the development of the second generation TAG-72 murine antibody CC49, which was evaluated for efficacy in Phase 2 clinical trials.³⁹ These trials evaluated an interferon adjuvant to enhance tumor antigen expression and ¹³¹I-labeled CC49 to target both soft tissue and bone metastases in hormone-resistant metastatic prostate cancer patients. The addition of the adjuvant therapy enhanced tumor uptake and anti-tumor effects of ¹³¹I-labeled CC49 alone based on a previous Phase 2 clinical trial of ¹³¹I-labeled CC49 in metastatic prostate cancer patients where pain relief was reported, but no objective antitumor response was observed.⁴⁰ While the experimental therapy was generally well tolerated, the results were modest, and disease progression was not delayed for more than 6 months. Moreover, human anti-mouse antibodies developed in all patients, which precluded repeat therapy by 8 weeks. It is possible that a humanized version of the murine CC49 may have improved efficacy. Regardless, therapeutic modalities have since shifted away from antibody-radionuclide conjugates toward ADCs.⁴¹ Advances in ADC formats are hypothesized to allow for more robust and durable results than previous murine radiotherapies because they utilize potent cytotoxic payloads instead of radionuclides.⁴²

With recent advances in ADC linker technology paired with various options in cytotoxic payloads, many new potential methods to target glycans are available. Variable immune responses exhibited in vaccine therapy can be circumvented by using ADCs with proper linker and payloads to achieve robust bystander killing in heterogeneous tumors. The payload used in our anti-STn ADC is MMAE, which is also the same payload incorporated in Adcetris[®], an FDA-approved drug for the treatment of Hodgkin lymphoma and systemic anaplastic large cell lymphoma.^{29,30} ADCs using the same payload format are currently in ongoing Phase 1/2 trials targeting solid tumors such as prostate, breast, lung, pancreatic, ovarian, and bladder.^{42,43} This toxin is shed at very low levels and is acceptable in safety assessments, with multiple MMAE ADC molecules having been evaluated for safety and toxicity in various clinical trials.⁴¹⁻⁴⁵ The ADC-linker technology used was the MC-vc-PAB-MMAE, a cleavable linker (CL) that allows for release of MMAE upon internalization into cells. MMAE is a membrane-permeable toxin that can be released from dying cells, resulting

in a bystander killing effect that produces greater efficacy in tumors with heterogeneous target expression.²⁸ STn expression is reported to be heterogeneous in stomach, colon, ovary, cervix, breast, and other carcinomas, with STn expression ranging from 5% to 100%.³ Another ADC-linker technology used was MMAF with a maleimidocaproyl (MC) linker. MMAF is a non-cell membrane permeable toxin and must be internalized to kill each tumor cell, thus it is ineffective in bystander killing. Based on the results of the COLO205 xenograft studies (Fig. 8), wherein S3F was compared with variations in ADC-linker technologies, MMAF resulted in no effects on tumor growth compared with controls. This may suggest bystander killing or the toxin/linker combination itself could be important for effective STn tumor targeting. Previously published studies with other targets using the MC-vc-PAB-MMAE system also demonstrated that bystander killing results in additional efficacy in heterogeneous tumors.²⁸ Understanding bystander killing and effects of the linker/toxin of our antibodies would be beneficial to their further characterization.

ADC binding to shed antigens can be a concern because these antigens act as a drug sink, effectively depleting therapeutic away from the intended tumor target. While shed STn has been reported to be present in the circulation, it has not been viewed as a limiting drug sink in related ADC clinical studies. STn in the serum and its effect as a possible drug sink have been described in the clinical study of an anti-MUC16 ADC (Genentech; Clinical Trials ID: NCT01335958).⁴⁶ MUC16 (CA125) is a known carrier of STn on cancer cells.⁴⁷ In this study, the circulating levels of CA125 had no effect on the pharmacokinetics of the anti-MUC16 ADC, even in patients with a high level of circulating CA125. This suggests that the soluble form of the drug target in blood may not result in a significant drug-sink effect.

A number of related TACAs have been preclinically validated. For example, an anti-Tn ADC⁴⁸ and MUC1-Tn CAR-T⁴⁹ have recently been evaluated. Tn, also known as CD175, is the non-sialylated form of STn. Tn is normally a building block for other complex sugars, and its expression is generally absent in normal adult tissues. Tn is expressed on cancer cell surfaces in a similar heterogeneous manner to STn when glycosylation is altered, particularly in metastatic lesions.⁴⁸ The anti-Tn-ADC, called Chi-Tn, is a chimeric antibody generated from an original murine IgM (83D4⁵⁰) that uses the MMAF payload, relying on cancer cell internalization for efficacy. While Chi-Tn demonstrated efficacy *in vitro* cytotoxic and *in vivo* xenograft models, its efficacy was only observed in high Tn-expressing models.⁴⁸ Chi-Tn did not demonstrate efficacy in these models when using cells with lower, more heterogeneous Tn expression, perhaps due to the absence of bystander killing with MMAF. In addition to ADC therapies, genetically modified T cells expressing chimeric antigen receptors (CARs) targeting Tn also have been described. A CAR-T targeting the glycoprotein MUC1 with the Tn modification was based upon the 5E5 MUC-Tn specific antibody. This therapy was described as effective in targeting T-cell lymphomas and pancreatic cancer in preclinical *in vitro* and *in vivo* models.⁴⁹

Our anti-STn antibodies target the glycan itself, not a specific glycopeptide, offering broad potential to bind multiple STn-glycosylated proteins on the surface of cancer cells. We

observed STn-specific reactivity across a wide array of solid epithelial tumor types. Our preliminary data shows striking reduction in tumor volumes in multiple *in vivo* models. Further development and humanization of our anti-STn ADC offers promise of effectively targeting this O-glycan modification in multiple cancers.

Materials and methods

Generation of STn specific antibodies

Mouse immunizations were used to generate a panel of anti-STn antibodies. Four mouse groups (N = 10 per group) were established using 6- to 8-week-old female BALB/c mice immunized with different antigens, but sharing the same adjuvant/immunization schedule to compare effectiveness of STn presenting antigens. All groups used AbISCO in combination with ODN-2395 as adjuvants to promote humoral as well as cellular immune responses. The first dose on Day 0 for all groups used 12 μ g AbISCO and 50 μ g ODN-2395. Unacceptable toxicity was evident with this strategy and the adjuvant doses for all subsequent boost regimes were reduced by half. Group 1 was immunized with 10 μ g porcine submaxillary mucin (PSM) on Days 0, 14, 28, and 42. Group 2 was immunized with alternating mucins: 10 μ g PSM on Day 0 and Day 28 and 10 μ g ovine submaxillary mucin (OSM) on Days 14 and 42. Group 3 was immunized with 10 μ g digested PSM on Days 0, 14, 28, and 42. Group 4 was immunized with OSM on Days 0, 14, 28, and 42. Each mouse was immunized with mucin/adjuvant subcutaneously (SC) around the armpits and inguinal regions (50 μ L per site, 4 sites, 200 μ L/mouse) on Days 0, 14, 28, and 42 as described above. Approximately 0.2 mL of whole blood was collected from mice on Days 0, 14, 28, 42, and 51 and processed for serum. Serum was screened for STn binding specificity using ELISAs and glycan arrays. Mice displaying desirable binding properties were immunized again with 10 μ g mucin (without adjuvants), 3 d later their immune response was probed by screening their sera. If the serum showed the desired robust and specific immune response, the corresponding mice were killed and their spleens were harvested and used for fusion to establish hybridomas and the anti-STn mouse antibody panel.

We used the HB-STn clone 3F1^{21,51} as a proof-of-concept for some studies. We class switched from a mouse IgG1 and recombinantly expressed this antibody as a mouse IgG2a; this engineered antibody is referred to as "S3F" in the text. B72.3 (ThermoFisher Scientific, catalog number MS138P), CC49 and 3H1951 (Santa Cruz Biotechnology, catalog numbers sc-20043 and sc-70558, respectively), STn219 (Abcam, catalog number ab115957) and MOPC173 (BioLegend, catalog number 400264) were used as assay controls.

Quantification of STn binding specificity ELISA

The antigens bovine (BSM), porcine (PSM) or ovine (OSM) submaxillary mucin were coated on Corning Costar high-binding plates (Corning, catalog number 9018) by overnight incubation of antigen solution in coating buffer (50 mM sodium carbonate/bicarbonate pH 9.5) at 4°C. When the sialic acid composition of these mucins is examined by HPLC, BSM

contains a mixture of Neu5Ac and Neu5Gc, while PSM contains mostly Neu5Gc, and OSM contains mainly Neu5Ac sialic acids (data not shown).⁵² After washing with phosphate-buffered saline (PBS), a subset of wells had their sialic acids oxidized by treatment with 2 mM periodate, wells were incubated for 20 minutes at 4°C. Plates were washed with 1x PBS and additional binding sites were blocked with 1% ovalbumin (OVA) in PBS for 1 hour. After a PBS wash, the anti-STn antibodies were added to wells in a serial dilution (0–100 nM), using 1% OVA as the diluent and were incubated for 2 hours at room temperature. Plates were washed 3 times with 0.05% Tween-20 –PBS followed by incubation with 0.08 μg/mL peroxidase-conjugated goat anti-mouse antibody (Jackson ImmunoResearch, catalog number 115–035–071) for 1 hour. Next, wells were washed 3 times with 0.05% Tween-20 –PBS and then wells were incubated with 100 μL of enzyme substrate (0.5 mg/mL o-phenylenediamine; 0.03% H₂O₂ in citric/phosphate buffer pH 5.5). The enzyme reaction was terminated by addition of an equal volume of 1.6 M sulfuric acid. Optical Density (OD) readings of periodate and non-periodate treated wells were determined at 490nm, log transformed and then fit to a nonlinear regression model (4-parameter logistic regression) to obtain a dose response curve. Data from periodate treated wells were subtracted from non-periodate treated wells to obtain the periodate-sensitive, STn binding curve and corresponding EC50 values. Binding affinities of anti-STn mouse mAbs were compared with the well-characterized mouse monoclonal anti-STn antibodies 3F1, B72.3 and CC49.

Qualification of STn specificity using glycan array

The glycan array was used to determine the glycan binding specificity of anti-STn antibodies. This array was developed in collaboration with Dr. Ajit Varki.³¹ STn and related glycans were synthesized and printed as described in the literature.³¹ Briefly, 71 glycans were synthesized using one-pot 3-enzyme chemoenzymatic approach;⁵³ structures were confirmed by DMB-HPLC, NMR or mass spectrometry. Glycans included 25 matched Neu5Ac/Gc pairs (including 9-O acetylated versions) along with several un-sialylated versions (Table S1). Glycans were diluted to a final concentration of 100 μM (300 mM phosphate buffer, pH 8.4) and printed in 4 replicates. Mouse whole IgG was printed at 0.05 μg/mL final concentration and printed in 4 replicates across the array matrix as a control. STn-specificity was determined comparing STn vs. non-STn glycan binding. Epoxy slides were blocked (0.1 M Tris, 0.05 M ethanol amine, pH 9.0) for 1 hour at 50°C. Slides were washed with distilled water, and blocked (PBS with 1% OVA) for 1 hour. Blocking buffer was aspirated and anti-STn antibody was added at 1 μg/mL concentration diluted in blocking buffer for 1 hour. Slides were washed twice with PBS with 0.1% Tween, then once with PBS alone. Next, secondary antibody (Cy3 goat anti-mouse, Jackson ImmunoResearch catalog number 115–165–071) was added at a final concentration 1.5 μg/mL in PBS for 1 hour. Slides were washed with PBS then distilled water and air-dried before reading on the GenePix 4000B (Molecular Devices). Fluorescence intensities were measured and background was subtracted using GenePix Pro software. Intensity of STn (Neu5Acα6GalNAcα and Neu5Gcα6GalNAcα), 9-O

acetylated STn (Neu5,9Ac2α6GalNAcα and Neu5-Gc9Acα6GalNAcα) and Tn (GalNAcα) were compared along with the remaining 66 glycans on the array. Binding was compared with mouse monoclonal anti-STn antibody 3F1, B72.3 and CC49.

Quantification of STn at the cell surface by flow cytometry

The binding affinities of anti-STn antibodies to STn on the surface of cells was determined by flow cytometry. Anti-STn antibodies were screened for binding to MDA-MB-231 cells stably transfected to express STn⁹ and absence of binding on non-STn expressing parental cells. Cells were harvested using Stem-ProAccutase buffer, cells were resuspended to a concentration of 5×10⁶ cells/mL in staining buffer (5% heat-inactivated fetal bovine serum in PBS). 50 μL of cells and 50 μL of staining buffer with anti-STn antibodies were combined. Antibodies were screened using a serial dilution over a concentration range of 0–300 nM. Antibodies and cells were incubated for 1 hour at 4°C. Cells were washed 3 times with staining buffer. Binding of antibodies was determined using an anti-mouse IgG allophycocyanin (APC)-conjugated secondary antibody at 1:1500 (Southern Biotech 1031–11L) diluted in staining buffer. A total of 5,000 events were acquired per sample using BD FACVerse and data was analyzed using FlowJo software. Mean of APC fluorescence and % APC positive cells were calculated. These data were log transformed then fit to a nonlinear regression model to obtain a dose response curve and EC50 binding calculations using Prism software. Mouse isotype MOPC173 antibody was used as an isotype control. The anti-epidermal growth factor receptor (EGFR) antibody LA22 (EMD Millipore catalog number 05–104) was used as a positive control.

Tumor microarray (TMA) – Immunohistochemistry analysis of STn expression

Commercially available FFPE TMAs containing a broad range of common human cancer specimens were scored microscopically by a qualified pathologist for antibody staining intensity, frequency and localization. Normal TMAs containing 60 samples (2 human donors each for 30 organs or subregions of organs, Super Bio Chips, Seoul, Korea, Product AC1), as well as common human cancer TMAs containing a total of 118 donor tumor samples (Super Bio Chips, Seoul, Korea, Products: MA2 and MA4), were immunohistochemically stained using 10 μg/mL of each candidate mAb using a standard ABC staining procedure following antigen retrieval. Cells and tissues known to either express, or not express STn were used as positive and negative control tissues, respectively. A total of 13 different common tumor types were tested overall, with numerous subclassification annotations captured for each tumor type. All commercially available human normal and cancer TMAs used in this study had been declassified by the manufacturer, and patient donors were not identifiable.

In vitro internalization assay

The pHAb amine reactive dye (Promega catalog number G9845) was conjugated to a subset of antibodies to determine

antibody internalization in MDA-MB-231 cells transfected to express STn⁹ and compared with non-expressing parental cells. Briefly, 0.2 mg/mL antibody was incubated with Protein A magnetic beads (IgG1 antibodies used Protein G instead) for 1 hour. Beads were washed, and a 20 molar excess of pHAb amine reactive dye was added and mixed for 1 hour. Beads were washed and bound antibody-pHAb was eluted and neutralized. The antibody recovery concentration and dye-to-antibody ratio was calculated according to the manufacturer's instructions. MDA-MB-231 STn⁺ and STn⁻ parental cells were seeded (4,000 cells/well) and allowed to incubate for 16 hours at 37°C before addition of 30 nM antibody-pHAb to media for overnight internalization at 37°C. The following day plates were washed with PBS and fluorescence was measured at ex/em 532 nm/560 nm. Wells treated with PBS only served as a measure of background fluorescence and were subtracted from pHAb experimental wells. Internalization of antibody-pHAb between STn⁺ and STn⁻ cells was compared using a 1-sided t-test with unequal variance and p-values along with Wilcoxon tests were performed on the data to determine significance.

Internalization was also visualized using Alexa-488 labeled anti-STn antibody S3F. Cells were incubated into Nunc Lab-Tek chamber slides and incubated overnight at 37°C. The next day, cells were incubated with 1, 5 or 10 µg/mL S3F-Alexa 488 at 4°C for 1 hour, washed once with ice cold PBS, then incubated with cell media at various times at 37°C (0, 15, 30, 60 minutes). After 37°C incubation, cells were treated with 5 minute acid wash (150 mM NaCl/HCl pH 2.5) to remove surface bound antibodies. Cells were then washed once with PBS, fixed for 15 minutes with 3% paraformaldehyde, 2% sucrose in PBS. Next, cells were washed once with PBS and counterstained with 1 µg/mL 4',6-diamidino-2-phenylindole for 5 minutes. Cells were then washed once with PBS, mounting medium was added (Vector H-1400) and slides were dried overnight. Images were collected on Nikon Eclipse Ti.

ADC conjugation

A subset of antibodies with promising binding attributes were conjugated to a cathepsin B-labile maleimidocaproyl-valine-citrulline-p-aminobenzyloxycarbonyl-monomethyl auristatin E (MC-vc-PAB-MMAE, referred to as CL-MMAE in the text). Additionally, *in vivo* potency comparison with S3F antibody conjugated to MMAF through a maleimidocaproyl (MC) linker (yielding Ab-MC-MMAF, referred to as NC-MMAF in the text). The inter-chain disulfide bonds of the antibodies were reduced and the maleimide linker was attached to the reduced cysteines. Conjugated antibodies were purified with a Sephadex G50 column; drug-antibody ratio (A248 nm/A280 nm) and conjugation efficiency was determined for each antibody.

In vitro antibody-drug-conjugated cytotoxicity

MDA-MB-231 STn transfected and parental STn⁻ cells were seeded at 2,000–4,000 cells/well and allowed to grow 16 hours before adding therapeutics. Conjugated anti-STn antibodies were added to wells at 0–50 nM (serial dilution). An irrelevant mouse isotype control and unconjugated antibodies were used as controls at the same concentrations. ADCs were incubated

with cells for 72 hours to generate a killing curve. Per manufacturer's instructions, Promega ADC CellTiter-Glo[®] Luminescent Cell Viability Assay kit (catalog number G7570) was used to determine the amount of ATP present, an indicator of metabolically active cells. An equal volume of CellTiter-Glo[®] Reagent was added directly to cell cultures. The addition of this reagent resulted in cell lysis and generation of a luminescent signal proportional to the amount of the number of live cells present in culture. Luminescent signal was determined and relative ADC potency was calculated, per the manufacturer's instructions to obtain percent viability and IC_{50s}.

In vivo xenograft ADC efficacy: MDA-MB-231 STn⁺

The anti-tumor activity of anti-STn ADCs were evaluated as single agents in a MDA-MB-231 STn⁺ human breast cancer xenograft model. This protocol was reviewed and approved by Translational Drug Development (TD2) (Scottsdale, AZ) Institutional Animal Care and Use Committee (IACUC) and in accordance with the National Institutes of Health Guide for the Care and Use of Laboratory Animals (NIH Publications No. 80–23, revised 1996). 5 × 10⁶ tumor cells were injected into the subcutaneous right flank (1:1 Matrigel:media mixture) into 5–8 week old female ICR SCID mice. Tumors were grown to a mean tumor size of 175–225 mm³, and mice were randomly equilibrated by tumor size into 6 groups. Mice were injected intraperitoneally (IP) with 2.5 mg/kg therapeutic antibodies (or vehicle only) once weekly for 3 weeks (Q7Dx3). Group 1 was vehicle control, group 2 was S3F-CL-MMAE, group 3 was 2G12-2B2-CL-MMAE, group 4 was 4G8-1E3-CL-MMAE, group 5 was isotype ADC control MOPC173-CL-MMAE, group 6 was an equal mixture of 2.5 mg/kg unconjugated 2G12-2B2 and 4G8-1E3. Therapeutic ADCs were diluted to appropriate concentration using vehicle control buffer (20 mM citrate + 150 mM NaCl). Tumor volume and body weight were calculated twice weekly and the study end point was when tumor volume exceeded 1000 mm³. Student t-test and %T/C were calculated along with growth curves and percent mouse weight changes to evaluate dose tolerance of the therapies.

In vivo xenograft ADC efficacy: COLO205

The anti-tumor activity of anti-STn ADCs were also evaluated as single agents in a COLO205 human colorectal cancer xenograft model. This protocol was reviewed and approved by the Translational Drug Development (TD2) IACUC and in accordance with the National Institutes of Health Guide for the Care and Use of Laboratory Animals (NIH Publications No. 80–23, revised 1996). 5 × 10⁶ tumor cells were injected subcutaneously into the right flank of 5–8 week old female athymic nude mice (1:1 Matrigel:media mixture). Tumors were grown to a mean size of 175–225 mm³, and mice were randomly equilibrated by tumor size into 4 groups – unconjugated S3F antibody, S3F-CL-MMAE (MC-vc-PAB-MMAE), S3F-NC-MMAF (MC-MMAF), or vehicle alone (20 mM citrate + 150 mM NaCl). Mice were IP dosed with 5 mg/kg therapeutic once weekly for 3 weeks (Q7Dx3).

Disclosure of potential conflicts of interest

This research may lead to the development of products which may be owned by and/or licensed to Siamab Therapeutics, Inc. in which JMP, DAE, MZ, and JB have a business and/or financial interest.

Acknowledgments

We would like to acknowledge Dr. Daniel T. Dransfield for his critical review of this manuscript and Dr. Kristen Starbuck for her technical contributions.

Funding

Research reported in this publication was supported in part by the National Cancer Institute (NCI) of the National Institutes of Health (NIH) Small Business Innovation Research (SBIR) under grants 1R43CA186326-01A1, HHSN261200700063C and HHSN261200900034C. The content is solely the responsibility of the authors and does not necessarily represent the official views of the NIH.

ORCID

Darius Ghaderi  <http://orcid.org/0000-0003-0542-7743>

References

- Siegel RL, Miller KD, Jemal A. Cancer statistics, 2016. *CA Cancer J Clin* 2016; 66:7-30. Available from: <http://www.ncbi.nlm.nih.gov/pubmed/26742998>; PMID:26742998; <http://dx.doi.org/10.3322/caac.21332>
- Christiansen MN, Chik J, Lee L, Anugraham M, Abrahams JL, Packer NH. Cell surface protein glycosylation in cancer. *Proteomics* 2014 [cited 2014 Oct 20]; 14:525-46. Available from: <http://www.ncbi.nlm.nih.gov/pubmed/24339177>; PMID:24339177; <http://dx.doi.org/10.1002/pmic.201300387>
- Julien S, Videira PA, Delannoy P. Sialyl-Tn in cancer: (how) did we miss the target? *Biomolecules* 2012 [cited 2013 Jan 28]; 2:435-66. Available from: <http://www.mdpi.com/2218-273X/2/4/435/>; PMID:24970145; <http://dx.doi.org/10.3390/biom2040435>
- Stowell SR, Ju T, Cummings RD. Protein glycosylation in cancer. *Annu Rev Pathol* 2015; 10:473-510. Available from: <http://www.ncbi.nlm.nih.gov/pubmed/25621663>; PMID:25621663; <http://dx.doi.org/10.1146/annurev-pathol-012414-040438>
- Hofmann BT, Schlüter L, Lange P, Mercanoglu B, Ewald F, Fölster A, Picksak A-S, Harder S, El Gammal AT, Grupp K, et al. COSMC knockdown mediated aberrant O-glycosylation promotes oncogenic properties in pancreatic cancer. *Mol Cancer* 2015; 14:109. Available from: <http://www.molecular-cancer.com/content/14/1/109>; PMID:26021314; <http://dx.doi.org/10.1186/s12943-015-0386-1>
- Pinho S, Marcos NT, Ferreira B, Carvalho AS, Oliveira MJ, Santos-Silva F, Harduin-Lepers A, Reis CA. Biological significance of cancer-associated sialyl-Tn antigen: modulation of malignant phenotype in gastric carcinoma cells. *Cancer Lett* 2007 [cited 2013 Jun 24]; 249:157-70. Available from: <http://www.ncbi.nlm.nih.gov/pubmed/16965854>; PMID:16965854; <http://dx.doi.org/10.1016/j.canlet.2006.08.010>
- Ozaki H, Matsuzaki H, Ando H, Kaji H, Nakanishi H, Ikehara Y, Narimatsu H. Enhancement of metastatic ability by ectopic expression of ST6GalNAcI on a gastric cancer cell line in a mouse model. *Clin Exp Metastasis* 2012 [cited 2013 Sep 19]; 29:229-38. Available from: <http://www.pubmedcentral.nih.gov/articlerender.fcgi?artid=3275730&tool=pmcentrez&rendertype=abstract>; PMID:22228572; <http://dx.doi.org/10.1007/s10585-011-9445-1>
- Julien S, Lagadec C, Krzewinski-Recchi M-A, Courtand G, Le Bourhis X, Delannoy P. Stable expression of sialyl-Tn antigen in T47-D cells induces a decrease of cell adhesion and an increase of cell migration. *Breast Cancer Res Treat* 2005; 90:77-84. Available from: <http://www.ncbi.nlm.nih.gov/pubmed/15770530>; PMID:15770530; <http://dx.doi.org/10.1007/s10549-004-3137-3>
- Julien S, Krzewinski-Recchi MA, Harduin-Lepers A, Gouyer V, Huet G, Le Bourhis X, Delannoy P. Expression of sialyl-Tn antigen in breast cancer cells transfected with the human CMP-Neu5Ac: GalNAc alpha2,6-sialyltransferase (ST6GalNAc I) cDNA. *Glycoconj J* 2001; 18:883-93. Available from: <http://www.ncbi.nlm.nih.gov/pubmed/12820722>; PMID:12820722; <http://dx.doi.org/10.1023/A:1022200525695>
- Häuselmann I, Borsig L. Altered tumor-cell glycosylation promotes metastasis. *Front Oncol* 2014 [cited 2014 Mar 6]; 4:28. Available from: <http://www.ncbi.nlm.nih.gov/pubmed/24592356>; PMID:24592356; <http://dx.doi.org/10.3389/fonc.2014.00028>
- Padler-Karavani V. Aiming at the sweet side of cancer: aberrant glycosylation as possible target for personalized-medicine. *Cancer Lett* 2014 [cited 2013 Oct 24]; 352:102-12. Available from: <http://www.ncbi.nlm.nih.gov/pubmed/24141190>; PMID:24141190; <http://dx.doi.org/10.1016/j.canlet.2013.10.005>
- Andergassen U, Liesche F, Kölbl AC, Ilmer M, Hutter S, Friese K, Jeschke U. Glycosyltransferases as markers for early Tumorigenesis. *Biomed Res Int* 2015; 2015:792672. Available from: <http://www.ncbi.nlm.nih.gov/pubmed/26161413>; PMID:26161413; <http://dx.doi.org/10.1155/2015/792672>
- Ju T, Wang Y, Aryal RP, Lehoux SD, Ding X, Kudelka MR, Cutler C, Zeng J, Wang J, Sun X, et al. Tn and sialyl-Tn antigens, aberrant O-glycomics as human disease markers. *Proteomics Clin Appl* 2013; 7:618-31. Available from: <http://www.ncbi.nlm.nih.gov/pubmed/23857728>; PMID:23857728; <http://dx.doi.org/10.1002/prca.201300024>
- Loureiro LR, Carrascal MA, Barbas A, Ramalho JS, Novo C, Delannoy P, Videira PA. Challenges in antibody development against Tn and Sialyl-Tn Antigens. *Biomolecules* 2015 [cited 2015 Dec 10]; 5:1783-809. Available from: <http://www.pubmedcentral.nih.gov/articlerender.fcgi?artid=4598775&tool=pmcentrez&rendertype=abstract>; PMID:26270678; <http://dx.doi.org/10.3390/biom5031783>
- Beatson R, Maurstad G, Picco G, Arulappu A, Coleman J, Wandell HH, Clausen H, Mandel U, Taylor-Papadimitriou J, Sletmoen M, et al. The breast cancer-associated Glycoforms of MUC1, MUC1-Tn and sialyl-Tn, are expressed in COSMC wild-type cells and bind the C-Type Lectin MGL. *PLoS One* 2015; 10:e0125994. Available from: <http://dx.plos.org/10.1371/journal.pone.0125994>; PMID:25951175; <http://dx.doi.org/10.1371/journal.pone.0125994>
- Carrascal MA, Severino PF, Guadalupe Cabral M, Silva M, Ferreira JA, Calais F, Quinto H, Pen C, Ligeiro D, Santos LL, Dall'olio F VP. Sialyl Tn-expressing bladder cancer cells induce a tolerogenic phenotype in innate and adaptive immune cells. *Mol Oncol* 2014; 8(3):753-65: S1574-7891-7; PMID:24656965; <http://dx.doi.org/10.1016/j.molonc.2014.02.008>
- Julien S, Picco G, Sewell R, Vercoutter-Edouart A-S, Tarp M, Miles D, Clausen H, Taylor-Papadimitriou J, Burchell JM. Sialyl-Tn vaccine induces antibody-mediated tumour protection in a relevant murine model. *Br J Cancer* 2009 [cited 2013 Jan 28]; 100:1746-54. Available from: <http://www.pubmedcentral.nih.gov/articlerender.fcgi?artid=2695689&tool=pmcentrez&rendertype=abstract>; PMID:19436292; <http://dx.doi.org/10.1038/sj.bjc.6605083>
- Miles D, Roché H, Martin M, Perren TJ, Cameron DA, Glaspy J, Dodwell D, Parker J, Mayordomo J, Tres A, et al. Phase III multicenter clinical trial of the sialyl-TN (STn)-keyhole limpet hemocyanin (KLH) vaccine for metastatic breast cancer. *Oncologist* 2011 [cited 2013 Feb 22]; 16:1092-100. Available from: <http://www.pubmedcentral.nih.gov/articlerender.fcgi?artid=3228158&tool=pmcentrez&rendertype=abstract>; PMID:21572124; <http://dx.doi.org/10.1634/theoncologist.2010-0307>
- Schlom J, Colcher D, Roselli M, Carrasquillo JA, Reynolds JC, Larson SM, Sugarbaker P, Tuttle SE, Martin EW. Tumor targeting with monoclonal antibody B72.3. *Int J Rad Appl Instrum B* 1989; 16:137-42. Available from: <http://www.ncbi.nlm.nih.gov/pubmed/2654088>; PMID:2654088; [http://dx.doi.org/10.1016/0883-2897\(89\)90184-0](http://dx.doi.org/10.1016/0883-2897(89)90184-0)
- Katari RS, Fernsten PD, Schlom J. Characterization of the shed form of the human tumor-associated glycoprotein (TAG-72) from serum

- effusions of patients with different types of carcinomas. *Cancer Res* 1990; 50:4885-90. Available from: <http://www.ncbi.nlm.nih.gov/pubmed/2379152>; PMID:2379152
21. Kjeldsen T, Clausen H, Hirohashi S, Ogawa T, Iijima H, Hakomori S. Preparation and characterization of monoclonal antibodies directed to the tumor-associated O-linked sialosyl-2-6 alpha-N-acetylglucosaminyl (sialosyl-Tn) epitope. *Cancer Res* 1988; 48:2214-20. Available from: <http://www.ncbi.nlm.nih.gov/pubmed/2450649>; PMID:2450649
 22. Cao Y, Stosiek P, Springer GF, Karsten U. Thomsen-Friedenreich-related carbohydrate antigens in normal adult human tissues: a systematic and comparative study. *Histochem Cell Biol* 1996; 106:197-207. Available from: <http://www.ncbi.nlm.nih.gov/pubmed/8877380>; PMID:8877380; <http://dx.doi.org/10.1007/BF02484401>
 23. Zhang S, Walberg LA, Ogata S, Itzkowitz SH, Koganty RR, Reddish M, Gandhi SS, Longenecker BM, Lloyd KO, Livingston PO. Immune sera and monoclonal antibodies define two configurations for the sialyl Tn tumor antigen. *Cancer Res* 1995; 55:3364-8. Available from: <http://www.ncbi.nlm.nih.gov/pubmed/7614472>; PMID:7614472
 24. McCluskie MJ, Weeratna RD, Evans DM, Makinen S, Drane D, Davis HL. CpG ODN and ISCOMATRIX adjuvant: a synergistic adjuvant combination inducing strong T-Cell IFN- γ responses. *Biomed Res Int* 2013; 2013:636847. Available from: <http://www.ncbi.nlm.nih.gov/pubmed/23586050>; PMID:23586050; <http://dx.doi.org/10.1155/2013/636847>
 25. Scott AM, Wolchok JD, Old LJ. Antibody therapy of cancer. *Nat Rev Cancer* 2012; 12:278-87. Available from: <http://www.ncbi.nlm.nih.gov/pubmed/22437872>; PMID:22437872; <http://dx.doi.org/10.1038/nrc3236>
 26. Hansel TT, Kropshofer H, Singer T, Mitchell JA, George AJT. The safety and side effects of monoclonal antibodies. *Nat Rev Drug Discov* 2010; 9:325-38. Available from: <http://www.ncbi.nlm.nih.gov/pubmed/20305665>; PMID:20305665; <http://dx.doi.org/10.1038/nrd3003>
 27. Oldham RK, Dillman RO. Monoclonal antibodies in cancer therapy: 25 years of progress. *J Clin Oncol* 2008; 26:1774-7. Available from: <http://www.ncbi.nlm.nih.gov/pubmed/18398141>; PMID:18398141; <http://dx.doi.org/10.1200/JCO.2007.15.7438>
 28. Li F, Emmerton KK, Jonas M, Zhang X, Miyamoto JB, Setter JR, Nicholas ND, Okeley NM, Lyon RP, Benjamin DR, et al. Intracellular released payload influences potency and bystander-killing effects of antibody-drug conjugates in preclinical models. *Cancer Res* 2016; 76:2710-9. Available from: <http://cancerres.aacrjournals.org/cgi/doi/10.1158/0008-5472.CAN-15-1795>; PMID:26921341; <http://dx.doi.org/10.1158/0008-5472.CAN-15-1795>
 29. Forero-Torres A, Holkova B, Goldschmidt J, Chen R, Olsen G, Boccia RV, Bordoni RE, Friedberg JW, Sharman JP, Palanca-Wessels MC, et al. Phase 2 study of frontline brentuximab vedotin monotherapy in Hodgkin lymphoma patients aged 60 years and older. *Blood* 2015; 126:2798-804. Available from: <http://www.bloodjournal.org/cgi/doi/10.1182/blood-2015-06-644336>; PMID:26377597; <http://dx.doi.org/10.1182/blood-2015-06-644336>
 30. Senter PD, Sievers EL. The discovery and development of brentuximab vedotin for use in relapsed Hodgkin lymphoma and systemic anaplastic large cell lymphoma. *Nat Biotechnol* 2012; 30:631-7. Available from: <http://www.nature.com/doi/10.1038/nbt.2289>; PMID:22781692; <http://dx.doi.org/10.1038/nbt.2289>
 31. Padler-Karavani V, Hurtado-Ziola N, Pu M, Yu H, Huang S, Muthana S, Chokhawa HA, Cao H, Secrest P, Friedmann-Morvinski D, et al. Human xeno-autoantibodies against a non-human sialic acid serve as novel serum biomarkers and immunotherapeutics in cancer. *Cancer Res* 2011 [cited 2013 Jan 28]; 71:3352-63. Available from: <http://www.pubmedcentral.nih.gov/articlerender.fcgi?artid=3085609&tool=pmcentrez&rendertype=abstract>; PMID:21505105; <http://dx.doi.org/10.1158/0008-5472.CAN-10-4102>
 32. Reuter G, Schauer R, Szeiki C, Kamerling JP, Vliegenthart JF. A detailed study of the periodate oxidation of sialic acids in glycoproteins. *Glycoconj J* 1989; 6:35-44. Available from: <http://www.ncbi.nlm.nih.gov/pubmed/2562505>; PMID:2562505; <http://dx.doi.org/10.1007/BF01047888>
 33. Yin Z, Chowdhury S, McKay C, Baniel C, Wright WS, Bentley P, Kaczanowska K, Gildersleeve JC, Finn MG, BenMohamed L, et al. Significant impact of immunogen design on the diversity of antibodies generated by carbohydrate-based anticancer vaccine. *ACS Chem Biol* 2015; 10:2364-72. Available from: <http://www.ncbi.nlm.nih.gov/pubmed/26262839>; PMID:26262839; <http://dx.doi.org/10.1021/acscchembio.5b00406>
 34. Ibrahim NK, Murray JL, Zhou D, Mittendorf EA, Sample D, Tautchin M, Miles D. Survival advantage in patients with metastatic breast cancer receiving endocrine therapy plus Sialyl Tn-KLH vaccine: post hoc analysis of a large randomized trial. *J Cancer* 2013; 4:577-84. Available from: <http://www.pubmedcentral.nih.gov/articlerender.fcgi?artid=3753533&tool=pmcentrez&rendertype=abstract>; PMID:23983823; <http://dx.doi.org/10.7150/jca.7028>
 35. Reddish M A, Jackson L, Koganty RR, Qiu D, Hong W, Longenecker BM. Specificities of anti-sialyl-Tn and anti-Tn monoclonal antibodies generated using novel clustered synthetic glycopeptide epitopes. *Glycoconj J* 1997; 14:549-60. Available from: <http://www.ncbi.nlm.nih.gov/pubmed/9298687>; PMID:9298687; <http://dx.doi.org/10.1023/A:1018576224062>
 36. Doerr RJ, Abdel-Nabi H, Krag D, Mitchell E. Radiolabeled antibody imaging in the management of colorectal cancer. Results of a multicenter clinical study. *Ann Surg* 1991; 214:118-24. Available from: <http://www.ncbi.nlm.nih.gov/pubmed/1867518>; PMID:1867518; <http://dx.doi.org/10.1097/00000658-199108000-00005>
 37. Bhatt P, Vhora I, Patil S, Amrutiya J, Bhattacharya C, Misra A, Mashru R. Role of antibodies in diagnosis and treatment of ovarian cancer: Basic approach and clinical status. *J Control Release* 2016; 226:148-67. Available from: <http://linkinghub.elsevier.com/retrieve/pii/S016836591630061X>; PMID:26860284; <http://dx.doi.org/10.1016/j.jconrel.2016.02.008>
 38. Schlom J, Colcher D, Siler K, Thor A, Bryant G, Johnston WW, Szpak CA, Sugarbaker P, Carrasquillo JA, Reynolds JC. Tumor targeting with monoclonal antibody B72.3: experimental and clinical results. *Cancer Treat Res* 1990; 51:313-35. Available from: <http://www.ncbi.nlm.nih.gov/pubmed/1977453>; PMID:1977453
 39. Meredith RF, Khazaeli MB, Macey DJ, Grizzle WE, Mayo M, Schlom J, Russell CD, LoBuglio AF. Phase II study of interferon-enhanced 131I-labeled high affinity CC49 monoclonal antibody therapy in patients with metastatic prostate cancer. *Clin Cancer Res* 1999; 5:3254s-3258s. Available from: <http://www.ncbi.nlm.nih.gov/pubmed/10541372>; PMID:10541372
 40. Meredith RF, Bueschen AJ, Khazaeli MB, Plott WE, Grizzle WE, Wheeler RH, Schlom J, Russell CD, Liu T, LoBuglio AF. Treatment of metastatic prostate carcinoma with radiolabeled antibody CC49. *J Nucl Med* 1994; 35:1017-22. Available from: <http://www.ncbi.nlm.nih.gov/pubmed/8195861>; PMID:8195861
 41. Kim EG, Kim KM. Strategies and advancement in antibody-drug conjugate optimization for targeted cancer therapeutics. *Biomol Ther (Seoul)* 2015; 23:493-509. Available from: <http://www.ncbi.nlm.nih.gov/pubmed/26535074>; PMID:26535074; <http://dx.doi.org/10.4062/biomolther.2015.116>
 42. Diamantis N, Banerji U. Antibody-drug conjugates—an emerging class of cancer treatment. *Br J Cancer* 2016; 114:362-7. Available from: <http://dx.doi.org/10.1038/bjc.2015.435>; PMID:26742008; <http://dx.doi.org/10.1038/bjc.2015.435>
 43. Perez HL, Cardarelli PM, Deshpande S, Gangwar S, Schroeder GM, Vite GD, Borzilleri RM. Antibody-drug conjugates: current status and future directions. *Drug Discov Today* 2014 [cited 2014 Jul 19]; 19:869-81. Available from: <http://linkinghub.elsevier.com/retrieve/pii/S135964461300398X>; PMID:24239727; <http://dx.doi.org/10.1016/j.drudis.2013.11.004>
 44. Yao X, Jiang J, Wang X, Huang C, Li D, Xie K, Xu Q, Li H, Li Z, Lou L, et al. A novel humanized anti-HER2 antibody conjugated with MMAE exerts potent anti-tumor activity. *Breast Cancer Res Treat* 2015; 153:123-33. Available from: <http://link.springer.com/10.1007/s10549-015-3503-3>; PMID:26253944; <http://dx.doi.org/10.1007/s10549-015-3503-3>
 45. Vacchelli E, Pol J, Bloy N, Eggermont A, Cremer I, Fridman WH, Galon J, Marabelle A, Kohrt H, Zitvogel L, et al. Trial watch: Tumor-

- targeting monoclonal antibodies for oncological indications. *Oncoimmunology* 2015; 4:e985940. Available from: <http://www.ncbi.nlm.nih.gov/pubmed/25949870>; PMID:25949870; <http://dx.doi.org/10.4161/2162402X.2014.985940>
46. Chen Y, Clark S, Wong T, Chen Y, Chen Y, Dennis MS, Luis E, Zhong F, Bheddah S, Koeppe H, et al. Armed antibodies targeting the mucin repeats of the ovarian cancer antigen, MUC16, are highly efficacious in animal tumor models. *Cancer Res* 2007; 67:4924-32. Available from: <http://www.ncbi.nlm.nih.gov/pubmed/17510422>; PMID:17510422; <http://dx.doi.org/10.1158/0008-5472.CAN-06-4512>
 47. Akita K, Yoshida S, Ikehara Y, Shirakawa S, Toda M, Inoue M, Kitawaki J, Nakanishi H, Narimatsu H, Nakada H. Different levels of sialyl-Tn antigen expressed on MUC16 in patients with endometriosis and ovarian cancer. *Int J Gynecol Cancer* 2012 [cited 2013 Oct 17]; 22:531-8. Available from: <http://www.ncbi.nlm.nih.gov/pubmed/22367369>; PMID:22367369; <http://dx.doi.org/10.1097/IGC.0b013e3182473292>
 48. Sedlik C, Heitzmann A, Viel S, Ait Sarkouh R, Batisse C, Schmidt F, De La Rochere P, Amzallag N, Osinaga E, Opezzo P, et al. Effective antitumor therapy based on a novel antibody-drug conjugate targeting the Tn carbohydrate antigen. *Oncoimmunology* 2016; 5:e1171434. Available from: <http://www.tandfonline.com/doi/full/10.1080/2162402X.2016.1171434>; PMID:27622021; <http://dx.doi.org/10.1080/2162402X.2016.1171434>
 49. Posey AD, Schwab RD, Boesteanu AC, Steentoft C, Mandel U, Engels B, Stone JD, Madsen TD, Schreiber K, Haines KM, et al. Engineered CAR T cells targeting the cancer-associated Tn-Glycoform of the membrane Mucin MUC1 control adenocarcinoma. *Immunity* 2016; 44:1444-54. Available from: <http://dx.doi.org/10.1016/j.immuni.2016.05.014>; PMID:27332733; <http://dx.doi.org/10.1016/j.immuni.2016.05.014>
 50. Osinaga E, Bay S, Tello D, Babino A, Pritsch O, Assemet K, Cantacuzene D, Nakada H, Alzari P. Analysis of the fine specificity of Tn-binding proteins using synthetic glycopeptide epitopes and a biosensor based on surface plasmon resonance spectroscopy. *FEBS Lett* 2000; 469:24-8. Available from: <http://www.ncbi.nlm.nih.gov/pubmed/10708749>; PMID:10708749; [http://dx.doi.org/10.1016/S0014-5793\(00\)01248-5](http://dx.doi.org/10.1016/S0014-5793(00)01248-5)
 51. Rajpert-De Meyts E, Poll SN, Goukasian I, Jeanneau C, Herlihy AS, Bennett EP, Skakkebaek NE, Clausen H, Giwercman A, Mandel U. Changes in the profile of simple mucin-type O-glycans and polypeptide GalNAc-transferases in human testis and testicular neoplasms are associated with germ cell maturation and tumour differentiation. *Virchows Arch* 2007 [cited 2013 Sep 19]; 451:805-14. Available from: <http://www.ncbi.nlm.nih.gov/pubmed/17694322>; PMID:17694322; <http://dx.doi.org/10.1007/s00428-007-0478-4>
 52. Hara S, Yamaguchi M, Takemori Y, Nakamura M, Ohkura Y. Highly sensitive determination of N-acetyl- and N-glycolylneuraminic acids in human serum and urine and rat serum by reversed-phase liquid chromatography with fluorescence detection. *J Chromatogr* 1986; 377:111-9. Available from: <http://www.ncbi.nlm.nih.gov/pubmed/3711202>; PMID:3711202; [http://dx.doi.org/10.1016/S0378-4347\(00\)80766-5](http://dx.doi.org/10.1016/S0378-4347(00)80766-5)
 53. Yu H, Chokhawala HA, Huang S, Chen X. One-pot three-enzyme chemoenzymatic approach to the synthesis of sialosides containing natural and non-natural functionalities. *Nat Protoc* 2006; 1:2485-92. Available from: <http://www.ncbi.nlm.nih.gov/pubmed/17406495>; PMID:17406495; <http://dx.doi.org/10.1038/nprot.2006.401>